OBSERVATIONS OF CHARGED PARTICLE PRECIPITATION OVER THE AURORAL ZONE DURING A MAGNETIC SUBSTORM*

by

K. L. Ackerson

Department of Physics and Astronomy
THE UNIVERSITY OF IOWA
Iowa City, Iowa

U. of Iowa 72-7

OBSERVATIONS OF CHARGED PARTICLE PRECIPITATION OVER THE AURORAL ZONE DURING A MAGNETIC SUBSTORM*

by

K. L. Ackerson

March, 1972

Department of Physics and Astronomy
The University of Iowa
Iowa City, Iowa 52240

*Research supported in part by the National Aeronautics and Space Administration under contracts NAS5-10625, NAS1-8141 and NAS1-2973 and grant NGL16-001-002 and by the Office of Naval Research under contract N000-14-68-A-0196-0003.

UNCLASSIFIED

Security Classification

DOCUMENT CONTROL DATA - R&D

(Security classification of title, body of abstract and indexing annotation must be entered when the overall report is classified)

1. ORIGINATING ACTIVITY (Corporate author) University of Iowa Department of Physics and Astronomy	2a. REPORT SECURITY CLASSIFICATION UNCLASSIFIED 2b. GROUP

3. REPORT TITLE

Observations of Charged Particle Precipitation Over the Auroral Zone During a Magnetic Substorm

4. DESCRIPTIVE NOTES (Type of report and inclusive dates)

5. AUTHOR(S) (Last name, first name, initial)

K. L. Ackerson

6. REPORT DATE March, 1972	7a. TOTAL NO. OF PAGES 33	7b. NO. OF REFS 23

8a. CONTRACT OR GRANT NO. N000-14-68-A-0196-0003 b. PROJECT NO. c. d.	9a. ORIGINATOR'S REPORT NUMBER(S) U. of Iowa 72-7 9b. OTHER REPORT NO(S) (Any other numbers that may be assigned this report)

10. AVAILABILITY/LIMITATION NOTICES

Distribution of this document is unlimited.

11. SUPPLEMENTARY NOTES	12. SPONSORING MILITARY ACTIVITY Office of Naval Research

13. ABSTRACT

SEE PAGES FOLLOWING

DD FORM 1 JAN 64 1473

UNCLASSIFIED

Security Classification

14 KEY WORDS	LINK A		LINK B		LINK C	
	ROLE	WT	ROLE	WT	ROLE	WT
Polar Magnetic Substorm						
Aurora						
Ring Current						
Plasma Sheet						

INSTRUCTIONS

1. ORIGINATING ACTIVITY: Enter the name and address of the contractor, subcontractor, grantee, Department of Defense activity or other organization *(corporate author)* issuing the report.

2a. REPORT SECURITY CLASSIFICATION: Enter the overall security classification of the report. Indicate whether "Restricted Data" is included. Marking is to be in accordance with appropriate security regulations.

2b. GROUP: Automatic downgrading is specified in DoD Directive 5200.10 and Armed Forces Industrial Manual. Enter the group number. Also, when applicable, show that optional markings have been used for Group 3 and Group 4 as authorized.

3. REPORT TITLE: Enter the complete report title in all capital letters. Titles in all cases should be unclassified. If a meaningful title cannot be selected without classification, show title classification in all capitals in parenthesis immediately following the title.

4. DESCRIPTIVE NOTES: If appropriate, enter the type of report, e.g., interim, progress, summary, annual, or final. Give the inclusive dates when a specific reporting period is covered.

5. AUTHOR(S): Enter the name(s) of author(s) as shown on or in the report. Enter last name, first name, middle initial. If military, show rank and branch of service. The name of the principal author is an absolute minimum requirement.

6. REPORT DATE: Enter the date of the report as day, month, year; or month, year. If more than one date appears on the report, use date of publication.

7a. TOTAL NUMBER OF PAGES: The total page count should follow normal pagination procedures, i.e., enter the number of pages containing information.

7b. NUMBER OF REFERENCES: Enter the total number of references cited in the report.

8a. CONTRACT OR GRANT NUMBER: If appropriate, enter the applicable number of the contract or grant under which the report was written.

8b, 8c, & 8d. PROJECT NUMBER: Enter the appropriate military department identification, such as project number, subproject number, system numbers, task number, etc.

9a. ORIGINATOR'S REPORT NUMBER(S): Enter the official report number by which the document will be identified and controlled by the originating activity. This number must be unique to this report.

9b. OTHER REPORT NUMBER(S): If the report has been assigned any other report numbers *(either by the originator or by the sponsor)*, also enter this number(s).

10. AVAILABILITY/LIMITATION NOTICES: Enter any limitations on further dissemination of the report, other than those imposed by security classification, using standard statements such as:

(1) "Qualified requesters may obtain copies of this report from DDC."

(2) "Foreign announcement and dissemination of this report by DDC is not authorized."

(3) "U. S. Government agencies may obtain copies of this report directly from DDC. Other qualified DDC users shall request through
_______________."

(4) "U. S. military agencies may obtain copies of this report directly from DDC. Other qualified users shall request through
_______________."

(5) "All distribution of this report is controlled. Qualified DDC users shall request through
_______________."

If the report has been furnished to the Office of Technical Services, Department of Commerce, for sale to the public, indicate this fact and enter the price, if known.

11. SUPPLEMENTARY NOTES: Use for additional explanatory notes.

12. SPONSORING MILITARY ACTIVITY: Enter the name of the departmental project office or laboratory sponsoring *(paying for)* the research and development. Include address.

13. ABSTRACT: Enter an abstract giving a brief and factual summary of the document indicative of the report, even though it may also appear elsewhere in the body of the technical report. If additional space is required, a continuation sheet shall be attached.

It is highly desirable that the abstract of classified reports be unclassified. Each paragraph of the abstract shall end with an indication of the military security classification of the information in the paragraph, represented as *(TS), (S), (C), or (U)*.

There is no limitation on the length of the abstract. However, the suggested length is from 150 to 225 words.

14. KEY WORDS: Key words are technically meaningful terms or short phrases that characterize a report and may be used as index entries for cataloging the report. Key words must be selected so that no security classification is required. Identifiers, such as equipment model designation, trade name, military project code name, geographic location, may be used as key words but will be followed by an indication of technical context. The assignment of links, roles, and weights is optional.

ABSTRACT

An array of sensitive electrostatic analyzers was launched on the satellite INJUN 5 into a nearly polar, low-altitude orbit. A series of three traversals of the northern auroral zone in the local evening sector on 3 December 1968 has provided high energy- and time-resolution observations of low-energy proton and electron intensities within the energy range $50 \le E \le 15{,}000$ eV before, during and after a polar magnetic substorm. The region of high intensities of plasma-sheet electrons expanded dramatically during the substorm, extending $\sim 3.5°$ farther poleward and $\sim 4.5°$ farther equatorward relative to that of the preceding pass. Electron number densities $\sim 1\ (cm^3\text{-}sr)^{-1}$ and energy fluxes ~ 5 ergs $(cm^2\text{-}sec\text{-}sr)^{-1}$ were observed both parallel and perpendicular to the local magnetic field in a region $\sim 9°$ in latitudinal width over the auroral zone. Ring-current protons with directional, integral intensities $\sim 4 \times 10^7\ (cm^2\text{-}sec\text{-}sr)^{-1}$ were injected to $L \sim 4.5$. It is concluded that the substorm was accompanied by a large-scale earthward motion and dissipation of the plasma sheet.

I. INTRODUCTION

The onset of a magnetospheric substorm near local midnight is manifested by many events including dramatic changes in the location and intensity of visible auroras and intense perturbations in the local magnetic field [see Akasofu, 1968, for a review]. Over the northern hemisphere the southernmost auroral arc, or a new arc south of the existing quiet arc, suddenly intensifies and spreads in all directions, forming the auroral bulge. Westward traveling surges associated with the rapid poleward expansion move toward dusk along existing quiet arcs.

Magnetic perturbations due to enhancement of the auroral electrojet are observed by stations near the auroral oval. Recently Kisabeth and Rostoker [1971] have presented an analysis of magnetic measurements with a line of stations along a magnetic meridian across the auroral zone. They find that the substorm onset near local midnight is marked by an abrupt increase of the current in the equatorward border of the electrojet. This portion of the electrojet remains relatively stable during the expansive phase of the substorm while strong enhancements of the current occur on the northern border of the electrojet. These enhancements, which are short-lived and may occur quasi-periodically, are thought to be associated with the passage of westward traveling surges. In consideration of the different time behavior and the spatial separation of the two components of the electrojet, Kisabeth and Rostoker suggest that their sources of energy "are different in character and probably in origin."

Several statistical studies of the properties of low-energy charged particle intensities over the auroral zone [Fritz and Gurnett, 1965; Sharp and Johnson, 1967, 1968; Craven, 1970; Hoffman, 1971] have provided significant results concerning the average character of auroral precipitation. It has recently been reported [Frank and Ackerson, 1972] that the trapping boundary for more energetic electrons, $E > 45$ keV, can be used often as a "natural coordinate" for detailed examination of low-energy charged particle intensities over the auroral ionosphere. Frank and Gurnett [1971] found that the trapping boundary separated a region of generally anti-sunward convection on the poleward side from a region of sunward convection on the equatorward side. On the basis of this and other plasma and plasma-wave measurements in the magnetosphere, the trapping boundary was interpreted as indicating the location of the high-latitude termination of closed field lines.

Frank and Ackerson [1972] found that the trapping boundary delineated the boundary between two populations of low-energy particles precipitating into the auroral ionosphere. During quiet times the primary energy input to the auroral zone during evening hours is usually due to electron "inverted V" events located poleward of the trapping boundary for energetic electron (E > 45 keV) intensities. The "inverted V" precipitation bands are characterized by increasing average electron energies to a maximum energy with a subsequent decrease in average energy as the satellite passes through these bands. In the early-morning sector, electrons of plasma sheet origin are observed equatorward of the trapping boundary as they drift eastward from their injection point in the local midnight sector. The "inverted V's" observed poleward of the trapping boundary in the morning sector are typically narrower and less energetic than their counterparts at local evening. In the vicinity of local midnight both types of precipitation are often seen.

In this paper we will examine a set of high energy- and time-resolution observations of low-energy proton and electron intensities over the late-evening auroral zone. These observations were obtained $\sim$ 2 hours before, during and $\sim$ 4 hours after a 300-γ negative bay was observed by the ground-based magnetometer at Great Whale River, Canada. Evidence will be presented that plasma-sheet electrons were being precipitated into the auroral zone over a region ~ 9° wide in invariant latitude during the substorm, compared to a band ~ 3° wide during the quiescent period preceding the substorm. Ring-current protons were injected deep (L ~ 4.5) into the outer zone simultaneously with the precipitation of electron intensities from the plasma sheet.

II. OBSERVATIONS

The data presented herein were obtained with an array of low-energy proton and electron differential energy analyzers (LEPEDEA'S) borne on the satellite INJUN 5 in a low-altitude polar orbit. The spacecraft was launched on 8 August 1968 with initial inclination of 80.7° and apogee and perigee altitudes of 2528 km and 677 km, respectively. Alignment of the spacecraft with the local magnetic field vector was maintained by means of two parallel, permanent bar magnets. Over the northern hemisphere the satellite was often commanded into a mode of operation with a telemetry rate of 24 kilobits per second. In this mode complete energy spectrums, each comprising 117 samples equally spaced logarithmically in energy, were obtained in 970 milliseconds simultaneously for both protons and electrons at local pitch angles of 0° and 90°. This cycle was repeated every two seconds. The differential energy spectrums measured by the LEPEDEA's spanned the energy ranges $50 \leq E \leq 15,000$ eV and $40 \leq E \leq 12,000$ eV for electrons and protons, respectively. Thin-windowed Geiger-Mueller tubes provided simultaneous measurements of more energetic electron intensities, $E > 45$ keV, at pitch angles of 0° and 90°. For further information concerning the spacecraft and instrumentation the reader may refer to Frank et al. [1966] and Frank and Ackerson [1971].

The observations of differential intensities of low-energy protons and electrons obtained with INJUN 5 are presented here in the form of E-t spectrograms. The ordinate of each spectrogram is particle energy in eV and the abscissa is Universal Time. The detector response at each point in the energy-time plane is color-coded from blue (low intensities) to red (high intensities). The color calibration strip along the right-hand side of the spectrogram is labeled with the $\log_{10}$ of the corresponding counting rate. Values for the invariant latitude (Λ), scalar magnetic field (B), and magnetic local time (MLT) at the satellite position are provided along the bottom of each spectrogram.

On 3 December 1968, between $\sim$ 0140 UT and $\sim$ 0740 UT, observations of low-energy charged particle intensities were obtained from three INJUN-5 traversals of the northern auroral zone. The latitude and longitude of the subsatellite point in geographic coordinates for the local late-evening portions of these three passes are shown in Figure 1. The magnetic local time of the satellite position for these observations was $\sim$ 22 hours.

Plotted above each of the subsatellite trajectories is the directional, integral energy flux in ergs $(cm^2\text{-sec-sr})^{-1}$ for precipitated electrons within the energy range $50 \leq E \leq 15{,}000$ eV. The locations of three magnetometer stations, Abisko (Sweden), Great Whale River (Canada) and College (Alaska), are also indicated on the map. Ancillary information concerning the three passes as well as the magnetic local times at the magnetic observatories for each of the passes is provided in Table I.

The location of the satellite orbit relative to the observatories and the time of the substorm with respect to the INJUN-5 traversal of the auroral oval provide us with an excellent series of low-altitude observations of proton and electron intensities before, during and after a substorm. Magnetograms from the three aforementioned stations showing the times (Table I) of the INJUN-5 auroral zone crossings are presented in Figures 2, 3 and 4. The feature of particular interest here is the $\sim$ 300-γ negative bay observed at Great Whale at 0345(±10) UT. This substorm was preceded by a magnetically quiet period although each of the three stations recorded some bay activity when it was last near local midnight. An examination of the magnetic coordinates for INJUN 5 and Great Whale during

TABLE I

Magnetic Indices, Satellite Altitudes and Magnetic Local Times for Ground Stations during INJUN-5 Substorm Observations on 3 December 1968

Revolution Number	U.T.	Altitude, kilometers	Dst*, gammas	Kp	MLT at: Abisko	Great Whale	College
1414	01^h45^m	2541	1	1^-	4.6^h	20.0^h	14.0^h
1415	03^h45^m	2537	-7, -21	4^+	6.4^h	22.2^h	16.1^h
1417	07^h40^m	2541	-20	3	11.0^h	2.5^h	20.4^h

* [Sugiura and Poros, 1971]

Revolution 1415 indicates that the point of closest approach to Great Whale of the trace of the magnetic field lines passing through the instantaneous positions of the satellite as projected to an altitude of 100 km was $\sim$ 150 km west of Great Whale River. This closest approach occurred at about 0347 UT, i.e., during the minimum in the negative bay. By $\sim$ 0735 UT, College had rotated to a point beneath the INJUN-5 trajectory. No magnetic activity was observed by the College magnetometer at the time of the satellite pass at 0733 to 0743 UT, although such activity was observed substantially later and commencing at $\sim$ 0830 UT.

Measurements of locally mirroring fluxes of energetic electrons, $E > 45$ keV, obtained with a thin-windowed Geiger-Mueller tube, for the three high-latitude passes are presented in Figure 5. The trapping boundary, defined as the high-latitude termination of measurable intensities of electrons with $E > 45$ keV, is easily identified for Revolutions 1414 and 1417 as being at $\Lambda \simeq 68.5°$ and $69.4°$ respectively. For Revolution 1415 the termination of measurable intensities of 45-keV electrons occurred at higher latitudes, $\Lambda \simeq 73.5°$.

Pre-Storm Observations.

Observations of precipitated electron intensities, $50 \leq E \leq 15{,}000$ eV, during Revolution 1414 are presented in the spectrogram on Plate 1. Two regions of narrow latitudinal extent and with low intensities of soft electrons were detected at 0142:26 and 0144:30 UT poleward of the trapping boundary. The trapping boundary was encountered at 0147:30 UT. At 0146:02 UT an integral intensity $\sim 3 \times 10^8$ electrons $(cm^2\text{-sec-sr})^{-1}$ was measured above the trapping boundary in a region $\sim$ 30 km in latitudinal width. The electron intensities in this region were isotropic to within instrumental accuracies, $\sim$ 25%, as measured at pitch angles of 0° and 90°. Integral intensities $\sim 5 \times 10^8$ electrons $(cm^2\text{-sec-sr})^{-1}$ with substantially harder electron spectrums, relative to their counterparts poleward of the trapping boundary, were observed at $\sim$ 0148 UT equatorward of the trapping boundary. Ring-current protons (not shown here) with energies greater than $\sim$ 5 keV were detected between $\sim$ 0147:40 and 0148:24 UT. These proton intensities were typical of those observed in the local late-evening sector during magnetically quiet times [see Plate 1b, Revolution 1487, Frank and Ackerson, 1972].

Six-second averages of several of the macroscopic parameters of the trapped and precipitated electron intensities are presented in Figure 6. These quantities were computed directly from the directional, differential intensities measured with the LEPEDEA'S. The number density, N, and energy density, W, are given in directional units.

Storm-Time Observations.

Approximately two hours later INJUN 5 again crossed the northern polar cap and intersected the late-evening auroral oval. A spectrogram of the precipitated electron intensities within the oval is presented on Plate 2. The observations between 0342 and $\sim$ 0344 UT were characteristic of the polar cap region on this pass. The intensities of protons and electrons within the energy range $50 \leq E \leq 15{,}000$ eV were below the instrumental threshold, $\leqslant 5 \times 10^6$ $(cm^2\text{-sec-sr})^{-1}$, over the trajectory from $\Lambda = 77°$ at 1300 MLT to the northern boundary of precipitation at $\sim$ 0344 UT (Plate 2). The onset of high intensities of electrons was very abrupt, with the responses at energies less than several keV rising by more than an order of magnitude within the time resolution of these observations (two seconds). The magnetic bay observed below the spacecraft at this time had already developed and was near its maximum intensity (Figure 3). The electron spectrums within the precipitation region were quite hard with significant intensities at energies above the instrumental upper limit of 15 keV. A series of electron spectrums for the time interval 0345:16 to 0346:00 UT is presented in Figure 7 [after Frank and Ackerson, 1971]. If the differential intensities for energies $E > 2$ keV are approximated with a spectrum of the form E^{-n}, values for n of ~ 1.4 to 2.0 are obtained. These intensities extrapolated to energies greater than 45 keV indicate that the electron spectrum is considerably steeper at these higher energies (see Figure 5).

A summary plot of six-second averages of the macroscopic parameters of the trapped and precipitated electron intensities is presented in Figure 8. Directional energy fluxes ~ 5 ergs $(cm^2\text{-sec-sr})^{-1}$ were observed over a band $\sim 9°$ invariant latitude in width. The electron intensities at pitch angles of 0° and 90° were equal, within factors ~ 2, during the entire traversal of the auroral zone.

In contrast to the electron intensities, the low-energy proton intensities displayed pitch-angle anisotropies which were markedly energy dependent. The spectrograms on Plates 3 and 4 summarize these observations of proton directional intensities at pitch angles 0° and 90°, respectively. Looking first at Plate 3 we see that measurable intensities of protons were first detected at

$\sim$ 0345:12 UT at energies $\sim$ 50 to 100 eV. This was $\sim$ 6 seconds after the minimum in the energetic electron intensities, E > 45 keV, at $\Lambda \simeq 71.6°$ was observed (see Figure 5) and was 68 seconds after the onset of high intensities of isotropic, lower energy electrons. The appearance of these proton intensities immediately preceded the hardening and intensification of the electron spectrum which commenced at 0345:18 UT. The maximum of proton intensities spanning the interval $\sim$ 0346 to 0349 UT was confined to a relatively narrow band of energies, the average value of which decreased from $\sim$ 1 keV to $\leq$ 60 eV during this 3-minute time period. A region of proton precipitation at all energies, $40 \leq E \leq 12{,}000$ eV, was observed between 0348:48 and 0349:18 UT. The equatorward termination of energetic proton precipitation may be associated with the position of the plasmapause; however, we have no direct means of determining the instantaneous position of the plasmapause.

Comparison of the trapped (Plate 4) with the precipitated (Plate 3) proton intensities indicates that the low-energy precursor ($\sim$ 0345 UT), the band with decreasing average energy (0346 to 0349 UT), and the energy-independent band at 0349 UT were all isotropic to within observational errors. However, the population of trapped protons with energies greater than several keV which first appeared at

$\sim$ 0347:30 UT (Plate 4) has no counterpart in Plate 3 (except for the isotropic region between 0348:48 and 0349:18 UT).

Values for the trapped and precipitated integral proton intensities ($J_\perp$ and $J_\parallel$) and the ratios $J_\perp/J_\parallel$ are presented in Figure 9. The anisotropy in the proton intensities is clearly visible starting at $\sim$ 0347:30 UT. The peak directional, integral intensities, $\sim 4 \times 10^7$ protons $(cm^2\text{-sec-sr})^{-1}$, and the directional energy densities, $\sim 1.5 \times 10^3$ eV $(cm^3\text{-sr})^{-1}$, for this pass are similar to those observed near the magnetic equator following the injection of the ring-current plasma during a magnetic storm [Frank, 1967b].

Post-Storm Observations.

The spectrogram for the precipitated electron intensities during Revolution 1417 (Plate 5) is typical of several of our other observations of low-energy electron intensities following substorm activity. The electron spectrums were soft relative to those observed during the substorm. The electron intensities were distributed over a greater latitudinal extent compared to those observed during periods of relative magnetic quiescence but had very similar energy spectrums. The spectral scans in the interval 0734:10 to 0734:18 UT and at 0735:02 UT were distorted due to loss of lock by a demodulator during processing of the telemetry, and are invalid. The electron spectrums for the "inverted V's" observed between 0734 and 0736 UT were much softer than the plasma-sheet spectrums for Revolution 1415, although the peak directional intensities, $\sim 2 \times 10^9$ electrons $(cm^2\text{-sec-sr})^{-1}$, were similar. These "inverted V" events were located well above the trapping boundary (encountered at 0738 UT). The electron number densities and directional intensities within the "inverted V" precipitation events (Figure 10) compare favorably with those reported by Frank and Ackerson [1972] for "inverted V's" during relatively quiet times. The electron intensities equatorward of the trapping boundary for this pass were also typical of the plasma-sheet intensities frequently observed in the local late-evening sector equatorward of the trapping boundary [Frank and Ackerson, 1972; Ackerson and Frank, 1972]. Comparable electron intensities have been observed at local late-evening in the plasma sheet in the vicinity of the magnetic equatorial plane [Schield and Frank, 1970; Frank, 1971].

Intensities of energetic ring-current protons were observed at $\sim$ 0739:30 UT, near the low-altitude termination of low-energy electron intensities at $L \sim 6.3$, and to lower latitudes through $\sim$ 0740:15 UT (spectrogram not shown here). These intensities were isotropic to within observational errors, factors ≤ 2. Somewhat higher intensities of trapped ring-current protons were encountered from 0741:30 UT ($L \sim 5.1$) until the end of telemetry at 0742:40 UT ($L \sim 4.5$). The directional intensities and energy densities for these protons were lower by factors of ~ 2 to 3 than those observed during the preceding substorm pass within the same latitude range.

III. DISCUSSION

On 3 December 1968 a series of high energy- and time-resolution observations of low-energy charged particle intensities over the northern auroral zone in the late-evening sector were obtained before, during and after a moderate magnetic bay. This fortuitous set of passes allowed direct comparison of the particle distributions present at three points in the temporal evolution of the substorm.

On the pass preceding the substorm the principal energy deposition occurred in a region $\sim 3°$ invariant latitudinal width located just equatorward of the trapping boundary for more energetic electrons, $E > 45$ keV. These low-energy electron intensities had spectrums and number densities similar to those observed at low latitudes in the near-earth plasma sheet [Schield and Frank, 1970], and were typical of other observations in the local late-evening sector during relatively quiet times [Frank and Ackerson, 1972]. However, usually "inverted V" bands poleward of or at the trapping boundary provide the dominant energy fluxes in this local time sector. Low intensities of ring-current protons were observed equatorward of and within the region of plasma-sheet electron intensities.

The next auroral zone crossing, $\sim$ 2 hours later, occurred during the minimum in a $\sim$ 300-γ negative bay observed beneath the spacecraft. The region of high intensities of low-energy electrons had expanded dramatically, extending $\sim$ 3.5° farther poleward and $\sim$ 4.5° farther equatorward than during the preceding pass. The trapping boundary had moved poleward and all significant precipitation was observed equatorward of the trapping boundary. More commonly during magnetically disturbed periods in the pre-midnight local time sector there will be at least one "inverted V" type event located poleward of the trapping boundary and the plasma-sheet electron intensities [Frank and Ackerson, 1971, 1972]. The directional electron number densities averaged $\sim 1\ (cm^3\text{-}sr)^{-1}$ during the auroral zone crossing and were generally isotropic over the upper hemisphere (see Figure 8). The directional electron energy density was $\sim 10^3$ eV $(cm^3\text{-}sr)^{-1}$. The peak proton directional energy density within the ring-current region was $\sim 1.5 \times 10^3$ eV $(cm^3\text{-}sr)^{-1}$. These values computed from the measurements of electron and proton intensities during Revolution 1415 compare favorably with the corresponding determinations reported by Frank [1967b] for magnetic-storm conditions at the magnetic equator and with the maximum values given by DeForest and McIlwain [1971] for the synchronous orbit at L = 6.6. Vasyliunas [1968] has also reported similar number densities and energy densities for low-energy electron intensities near the magnetic equator during substorms. The substorm energy spectrums of the electron intensities were quite hard compared to those observed preceding the substorm. A power-law spectral form, E^{-n}, with $n \sim 1.4$ to 2.0 provided a good fit for $E > 2$ keV. While the high-energy tail, $2 < E < 15$ keV, of these spectrums was harder than those usually detected in the quiescent plasma sheet, they are similar to those sometimes found during disturbed periods [Frank, 1967a; Montgomery, 1968]. There is thus strong evidence that the charged particle intensities at low altitudes during Revolution 1415 are directly associated with those of the plasma sheet. The large latitudinal extent of the region indicates that this relatively short-lived precipitation event was due to a rapid earthward motion and collapse of the plasma sheet. This conclusion is in agreement with those reached by numerous previous researches [cf. Axford, 1969, and references therein].

An examination of the magnetograms from Great Whale River shows that the INJUN-5 auroral zone crossing occurred during a time of large fluctuations in the auroral current systems. However, the spacecraft velocity ($\sim$ 6.3 km/sec) was sufficiently greater than the typical apparent velocities of auroral forms ($\lesssim$ 1 km/sec) reported by Akasofu

[1968] that we do not feel the overall spatial distributions reported above were substantially affected by temporal variations during the auroral zone traversal.

Kisabeth and Rostoker [1971] examined a number of polar magnetic substorms with a meridional chain of magnetic observatories. They concluded that there are generally two distinct current systems associated with a substorm, one on the southern edge of the electrojet whose development characterizes the initial phase of the substorm, and a second current system on the northern border of the electrojet, the intensification of which is thought to be associated with a westward traveling surge. These current systems have been observed to merge on occasion forming a single current system as much as $\sim 10°$ in latitudinal width. It is noteworthy to compare these results with further INJUN-5 measurements of low-energy electron precipitation patterns over the auroral zone. During disturbed periods we find typically one or more "inverted V" events poleward of the trapping boundary [Frank and Ackerson, 1971; Ackerson and Frank, 1972]. Figure 11 presents an example of a series of observations of a narrow plasma "hole" separating an "inverted V" structure from the plasma-sheet electron intensities. This narrow region of markedly low energy fluxes was detected at 70.4°(±0.5°) invariant latitude on the three consecutive INJUN-5 auroral zone crossings while the peak directional electron energy fluxes within the "inverted V's" varied from ∼ 80 ergs $(cm^2\text{-sec-sr})^{-1}$ on Revolution 1644 to ∼ 0.08 ergs $(cm^2\text{-sec-sr})^{-1}$ on Revolution 1645 and to ∼ 8 ergs $(cm^2\text{-sec-sr})^{-1}$ on Revolution 1646. Such narrow regions of negligible electron precipitation were not at all uncommon in our observations of auroral zone precipitation patterns in the local late-evening sector. In the limited number of cases where telemetry was available for consecutive auroral zone crossings, it appeared that the invariant latitude of the "hole" was approximately constant to within several degrees provided no substorm events of the type observed on Revolution 1415 occurred. While the evidence is by no means conclusive, it suggests that the northern current system proposed by Kisabeth and Rostoker may well be associated with the "inverted V" events observed poleward of the trapping boundary by INJUN 5 and the southern system associated with the plasma sheet positioned equatorward of the trapping boundary. Events such as that encountered during Revolution 1415 almost certainly result from a large-scale collapse of the plasma sheet and the associated enhancement of convection. They are infrequently encountered in our observations as would be expected of a magnetospheric configuration with a short lifetime and a low frequency of occurrence.

The proton intensities during the storm-time auroral zone crossing displayed a complex structure. Measurable intensities of precipitating protons were observed in a region $\sim 8°$ invariant latitude in width, within the region containing plasma-sheet electron intensities. These proton intensities spanned a larger latitudinal zone and penetrated to lower latitudes relative to those of the pre-storm measurements. Cornwall et al. [1970; 1971] have proposed a mechanism for the turbulent dissipation of the ring-current proton intensities at the plasmapause as the plamasphere expands following a magnetic storm. If such a ring current-plasmasphere interaction was responsible for the isotropic intensities of protons observed at $\sim$ 0349 UT (Figure 9 and Plates 3 and 4), the region containing the higher densities of these low-energy protons had a corresponding equatorial thickness of $\sim$ 0.3 earth radius.

Our present observations provide a detailed examination of the particle intensities over the auroral zone before, during and after a magnetic substorm. However, since the orbital period of a low-altitude satellite is similar to the time scale of a substorm we can obtain relatively few "snapshots" of the relevant auroral-zone precipitation patterns. Further investigations of the substorm triggering mechanism and of the local-time development of a substorm, at higher temporal resolution during a single substorm, are largely obviated if measurements from only one low-altitude satellite are employed. Accordingly, we are currently undertaking correlative studies using several satellites at widely separated points to continue this study of the temporal evolution of substorms and their relationships to plasma phenomena within the magnetosphere.

ACKNOWLEDGMENT

The author is grateful to Professor L. A. Frank for his many discussions and helpful comments concerning this research. The magnetograms in this paper were obtained through the services of Mr. William Paulishak, World Data Center A, Rockville, Maryland. This research was supported in part by the National Aeronautics and Space Administration under contracts NAS5-10625, NAS1-8141 and NAS1-2973 and grant NGL16-001-002 and by the Office of Naval Research under contract N000-14-68-A-0196-0003.

References

Ackerson, K. A., and L. A. Frank, Correlated satellite measurements of low-energy electron precipitation and ground-based observations of a visible auroral arc, J. Geophys. Res., 77, 1128, 1972.

Akasofu, S.-I., Polar and Magnetospheric Substorms, D. Reidel, Dordrecht-Holland, 1968.

Axford, W. I., Magnetospheric convection, Rev. Geophys., 7, 421, 1969.

Cornwall, J. M., F. V. Coroniti, and R. M. Thorne, Turbulent loss of ring current protons, J. Geophys. Res., 75, 1279, 1970.

Cornwall, J. M., F. V. Coroniti, and R. M. Thorne, Unified theory of SAR arc formation at the plasmapause, J. Geophys. Res., 76, 4428, 1971.

Craven, J. D., A survey of low-energy (E $\geqslant$ 5 keV) electron energy fluxes over the northern auroral regions with satellite Injun 4, J. Geophys. Res., 75, 2468, 1970.

DeForest, S. E., and C. E. McIlwain, Plasma clouds in the magnetosphere, J. Geophys. Res., 76, 3587, 1971.

Frank, L. A., Initial observations of low-energy electrons in the earth's magnetosphere with OGO 3, J. Geophys. Res., 72, 185, 1967a.

Frank, L. A., On the extraterrestrial ring current during geomagnetic storms, J. Geophys. Res., 72, 3753, 1967b.

Frank, L. A., Relationship of the plasma sheet, ring current, trapping boundary, and plasmapause near the magnetic equator and local midnight, J. Geophys. Res., 76, 2265, 1971.

Frank, L. A., and K. L. Ackerson, Observations of charged particle precipitation into the auroral zone, J. Geophys. Res., 76, 3612, 1971.

Frank, L. A., and K. L. Ackerson, Local-time survey of plasma at low altitudes over the auroral zones, J. Geophys. Res., (accepted for publication), 1972.

Frank, L. A., and D. A. Gurnett, Distributions of plasmas and electric fields over the auroral zones and polar caps, J. Geophys. Res., 76, 6829, 1971.

Frank, L. A., W. W. Stanley, R. H. Gabel, D. C. Enemark, R. F. Randall, and N. K. Henderson, Technical description of LEPEDEA instrumentation (Injun 5), Univ. of Iowa Res. Rep. 66-31, Iowa City, 1966.

Fritz, T. A., and D. A. Gurnett, Diurnal and latitudinal effects observed for 10-keV electrons at low satellite altitudes, J. Geophys. Res., 70, 2485, 1965.

Hoffman, R. A., Auroral electron drift and precipitation: cause of the mantle aurora, _J. Geophys. Res._, (submitted for publication), 1971.

Kisabeth, J. L., and G. Rostoker, Development of the polar electrojet during polar magnetic substorms, _J. Geophys. Res._, _76_, 6815, 1971.

Montgomery, M. D., Observations of electrons in the earth's magnetotail by Vela Launch 2 satellites, _J. Geophys. Res._, _73_, 871, 1968.

Schield, M. A., and L. A. Frank, Electron observations between the inner edge of the plasma sheet and the plasmasphere, _J. Geophys. Res._, _75_, 5401, 1970.

Sharp, R. D., R. G. Johnson, M. F. Shea, and G. B. Shook, Satellite measurements of precipitating protons in the auroral zone, _J. Geophys. Res._, _72_, 227, 1967.

Sharp, R. D., and R. G. Johnson, Some average properties of auroral electron precipitation as determined from satellite observations, _J. Geophys. Res._, _73_, 969, 1968.

Sugiura, M., and D. J. Poros, Hourly values of equatorial Dst for the years 1957 to 1970, _Goddard Space Flight Center Preprint X-645-71-278_, 1971.

Vasyliunas, V. M., A survey of low-energy electrons in the evening sector of the magnetosphere with OGO 1 and OGO 3, _J. Geophys. Res._, _73_, 2839, 1968.

Figure Captions

Plate 1. A color-coded energy-time spectrogram for precipitated electron intensities over the northern auroral zone in the local evening sector on 3 December 1968. This pass occurred ~ 2 hours prior to a ~ 300-γ substorm. The ordinate and abscissa are electron energy and Universal Time, respectively, with the detector response at a point on the E-t plane color-coded from blue (low intensities) to red (high intensities).

Plate 2. Continuation of Plate 1 for precipitated electron intensities over Great Whale River during a ~ 300-γ substorm. Similar electron intensities were observed at local pitch angles of 90°. Directional electron energy fluxes $\geq$ 5 ergs $(cm^2\text{-sec-sr})^{-1}$ were observed in a band ~ 9° invariant latitude in width.

Plate 3. Continuation of Plate 2 for precipitated proton intensities during the substorm.

Plate 4. Continuation of Plate 2 for trapped proton intensities during the substorm. Peak integral, directional intensities ~ 4×10^7 $(cm^2\text{-sec-sr})^{-1}$ were observed within the ring-current region at ~ 0347-0350 UT.

Plate 5. Continuation of Plate 1 for precipitated electron intensities over the northern auroral zone following the substorm.

Figure 1. Plots of the geocentric latitude and longitude for the three INJUN-5 traversals of the auroral zone during 3 December 1968. Plotted above each track are the directional electron energy fluxes in ergs $(cm^2\text{-sec-sr})^{-1}$ observed during each pass. The magnetic local time for each of the passes was approximately 22^h.

Figure 2. Magnetogram from College, Alaska for the first eight hours of 3 December 1968. The times of the three INJUN-5 auroral zone traversals are indicated by vertical lines at 0145, 0345 and 0740 UT.

Figure 3. Continuation of Figure 2 for Great Whale River, Canada. At 0347 UT the subsatellite point passed within $\sim$ 150 km of the magnetic meridian of Great Whale River.

Figure 4. Continuation of Figure 2 for Abisko, Sweden.

Figure 5. Directional intensities of trapped electrons, $E > 45$ keV, as functions of invariant latitude for the three passes at $\sim 22^h$ magnetic local time on 3 December 1968.

Figure 6. Six-second averages of several plasma parameters computed from observations of directional, differential electron intensities over the northern auroral zone during Revolution 1414. The units of each of the quantities are as follows: J, electrons $(cm^2\text{-sec-sr})^{-1}$; F, ergs $(cm^2\text{-sec-sr})^{-1}$; N, electrons $(cm^3\text{-sr})^{-1}$; W, eV $(cm^3\text{-sr})^{-1}$; $< E >$, eV.

Figure 7. Several sample directional, differential energy spectrums of precipitated electron intensities for the E-t spectrogram from Revolution 1415 (Plate 2). The ordinate scale for each consecutive spectrum has been displaced by a factor of 10 [after Frank and Ackerson, 1971].

Figure 8. Continuation of Figure 6 for Revolution 1415. A 300-γ magnetic substorm was observed beneath the spacecraft at Great Whale River.

Figure 9. High-temporal resolution observations of the directional, integral trapped ($J_\perp$) and precipitated ($J_\parallel$) proton intensities and the ratios, $J_\perp/J_\parallel$, observed at local evening during the substorm (cf. Plates 3 and 4).

Figure 10. Continuation of Figure 6 for Revolution 1417 following the substorm.

Figure 11. Precipitated electron energy flux as a function of invariant latitude for a series of three traversals of the auroral zone at local evening on 21-22 December 1968. For each of the passes the minimum in the precipitated electron intensities located at $\Lambda = 70.4°$ (±0.5°) separated an "inverted V" band (poleward) from a region of plasma-sheet electron intensities (equatorward). This narrow plasma "hole" was observed at nearly the same invariant latitude during the three passes while the peak electron energy fluxes within the "inverted V" events varied from 80 ergs $(cm^2\text{-}sec\text{-}sr)^{-1}$ to 0.08 ergs $(cm^2\text{-}sec\text{-}sr)^{-1}$ to 8 ergs $(cm^2\text{-}sec\text{-}sr)^{-1}$ for Revolutions 1644, 1645 and 1646, respectively.

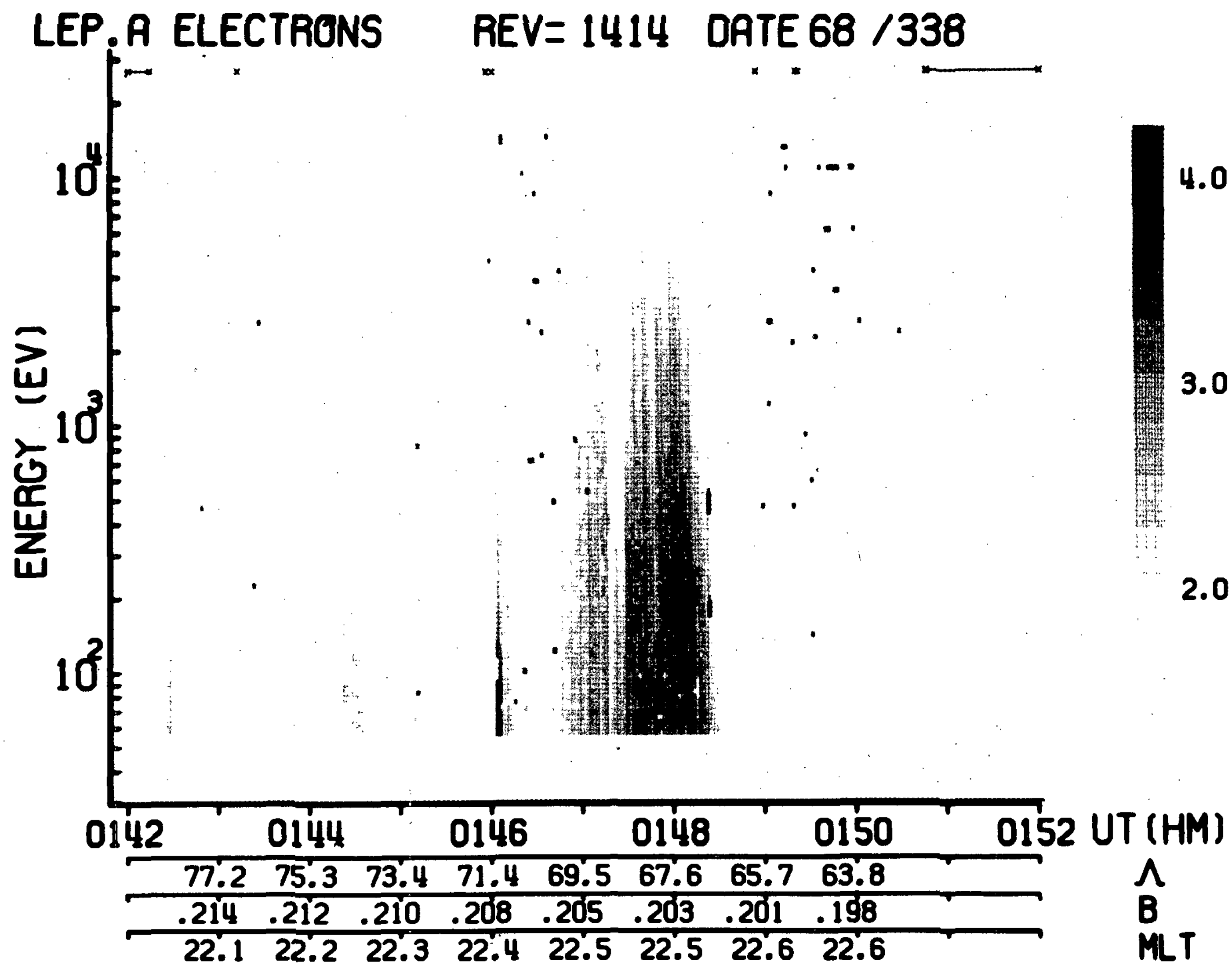
LEP.A ELECTRONS REV= 1414 DATE 68 /338
ENERGY (EV)
10^4
10^3
10^2
4.0
3.0
2.0
0142
0144
0146
0148
0150
0152
UT (HM)
77.2 75.3 73.4 71.4 69.5 67.6 65.7 63.8
Λ
.214 .212 .210 .208 .205 .203 .201 .198
B
22.1 22.2 22.3 22.4 22.5 22.5 22.6 22.6
MLT

Plate 1.

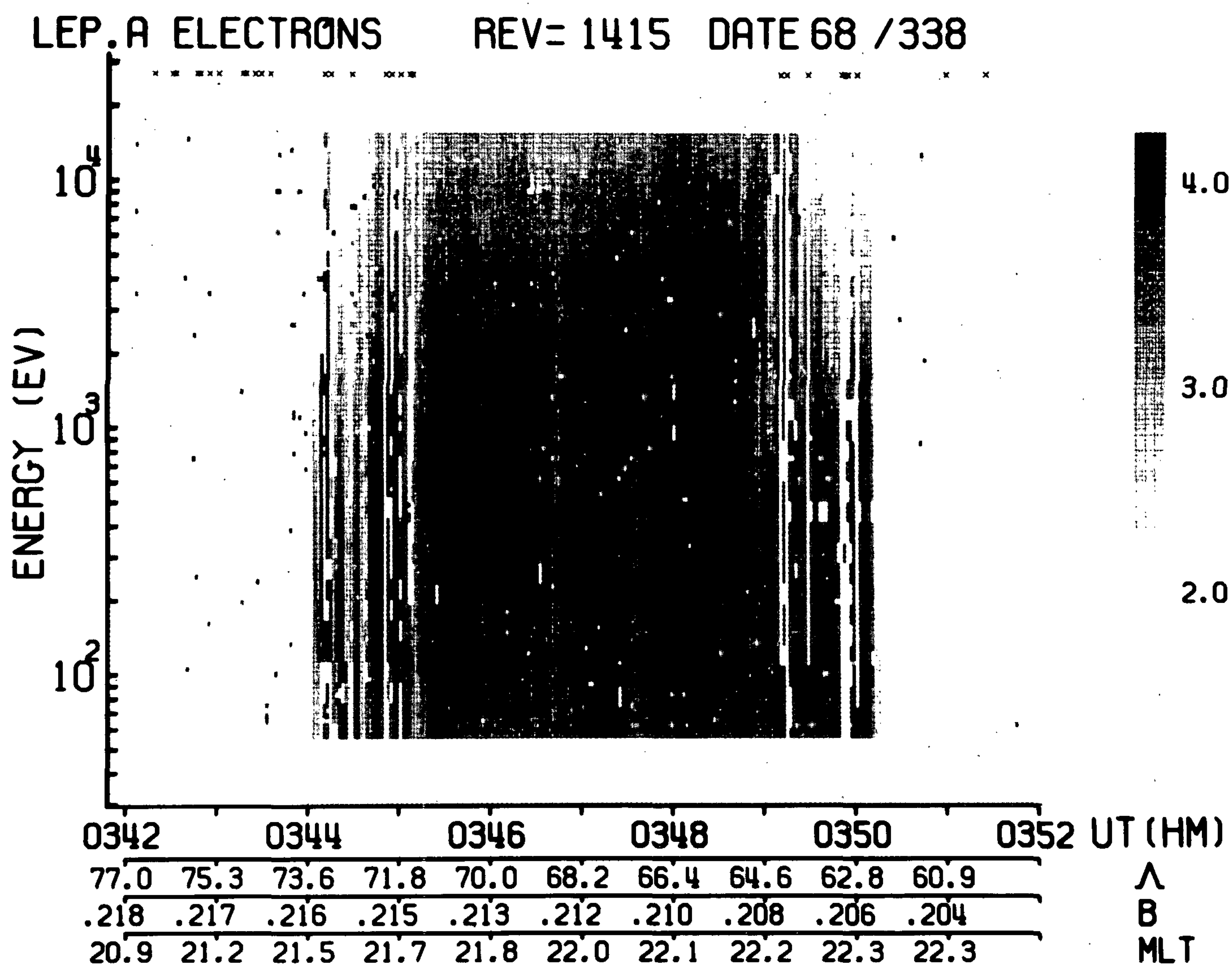
LEP.A ELECTRONS REV= 1415 DATE 68 /338
ENERGY (EV)
10^4
10^3
10^2
4.0
3.0
2.0
0342
0344
0346
0348
0350
0352 UT (HM)
77.0 75.3 73.6 71.8 70.0 68.2 66.4 64.6 62.8 60.9 Λ
.218 .217 .216 .215 .213 .212 .210 .208 .206 .204 B
20.9 21.2 21.5 21.7 21.8 22.0 22.1 22.2 22.3 22.3 MLT

Plate 2.

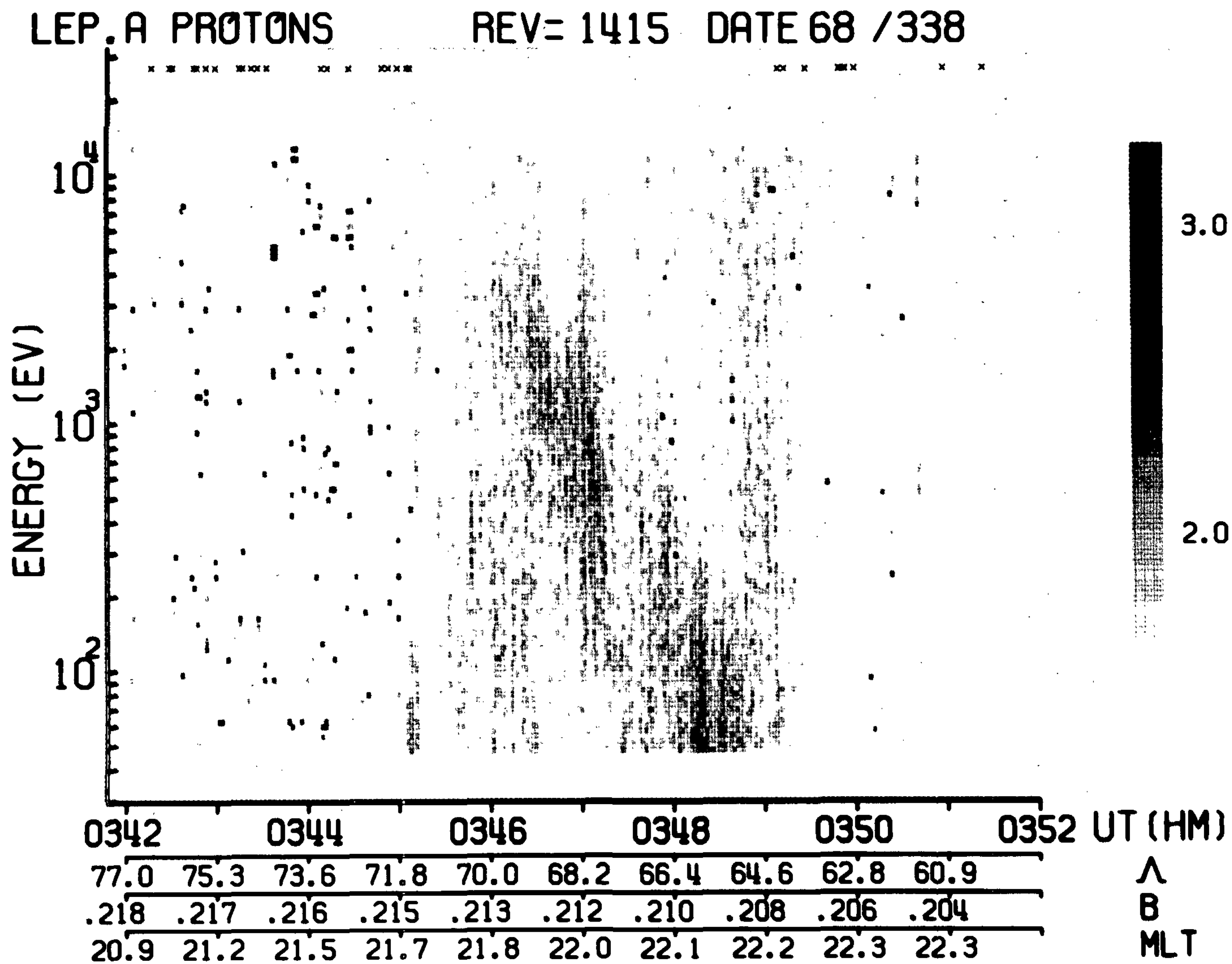
LEP.A PROTONS
REV= 1415 DATE 68 /338
ENERGY (EV)
10^4
10^3
10^2
3.0
2.0
0342
0344
0346
0348
0350
0352
UT (HM)
77.0 75.3 73.6 71.8 70.0 68.2 66.4 64.6 62.8 60.9
Λ
.218 .217 .216 .215 .213 .212 .210 .208 .206 .204
B
20.9 21.2 21.5 21.7 21.8 22.0 22.1 22.2 22.3 22.3
MLT

Plate 3.

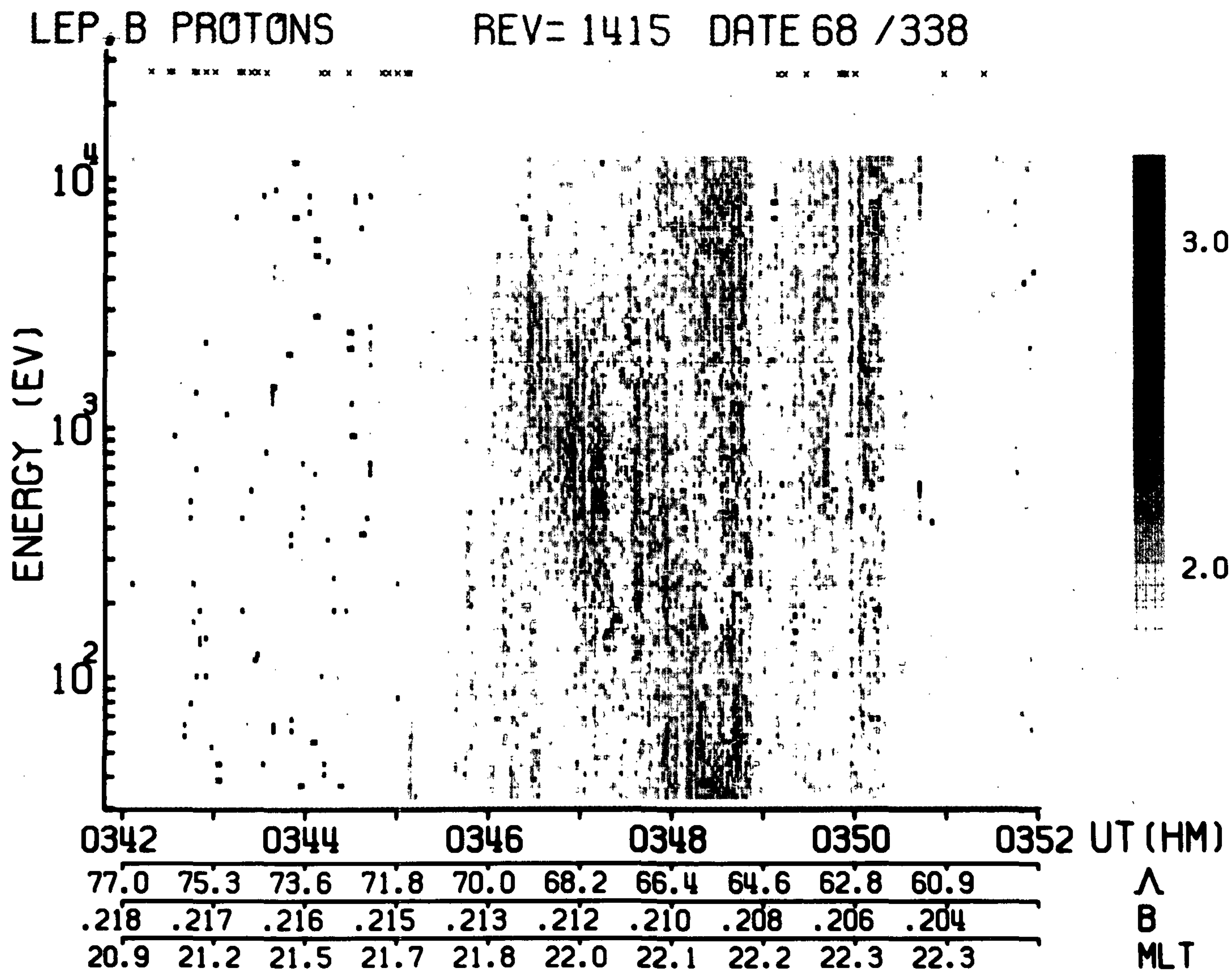
LEP.B PROTONS
REV= 1415 DATE 68 /338
ENERGY (EV)
10^4
10^3
10^2
3.0
2.0
0342
0344
0346
0348
0350
0352
UT (HM)
77.0 75.3 73.6 71.8 70.0 68.2 66.4 64.6 62.8 60.9
Λ
.218 .217 .216 .215 .213 .212 .210 .208 .206 .204
B
20.9 21.2 21.5 21.7 21.8 22.0 22.1 22.2 22.3 22.3
MLT

Plate 4.

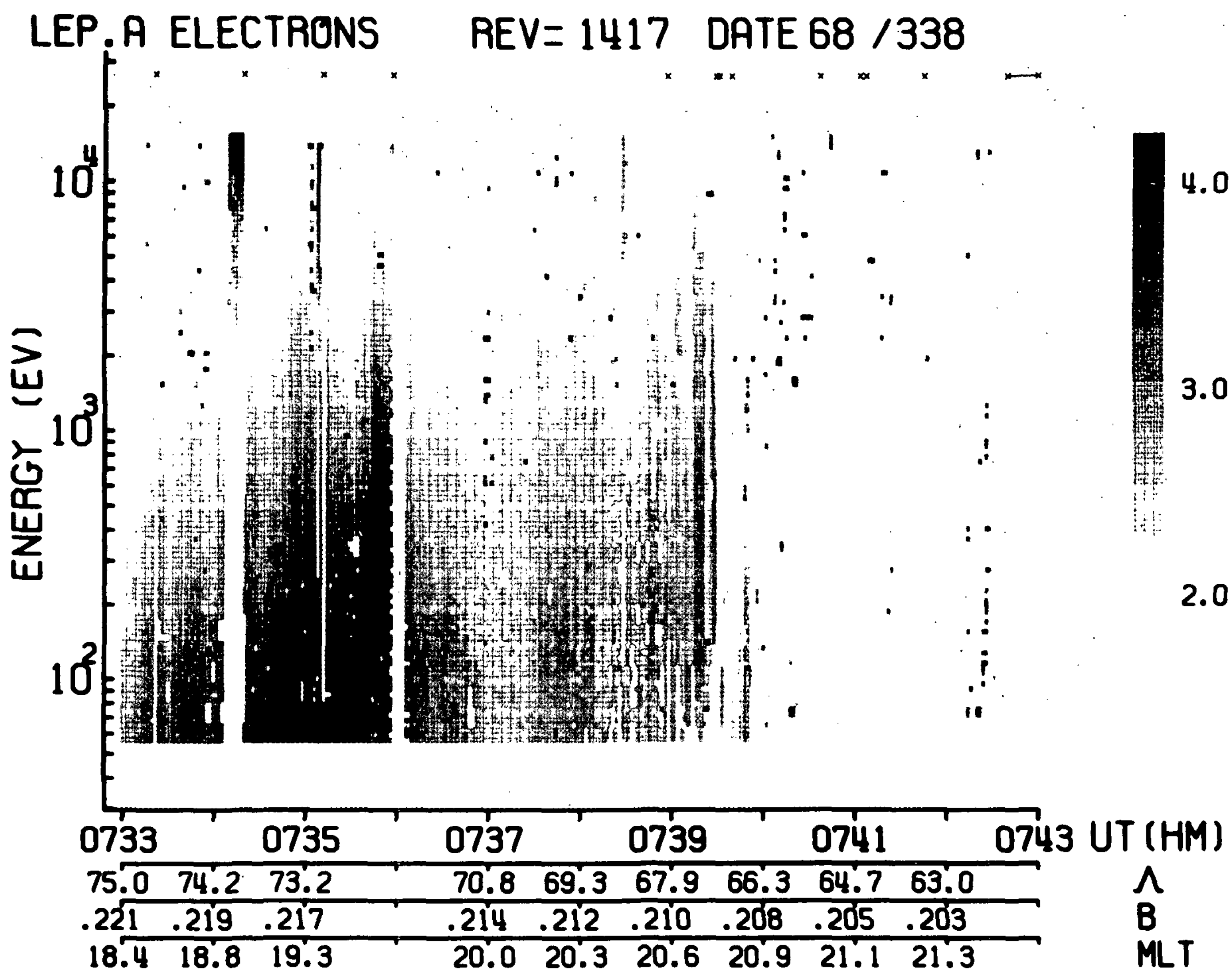
LEP.A ELECTRONS REV= 1417 DATE 68 /338
ENERGY (EV)
10^4
10^3
10^2
4.0
3.0
2.0
0733 0735 0737 0739 0741 0743 UT (HM)
75.0 74.2 73.2 70.8 69.3 67.9 66.3 64.7 63.0 Λ
.221 .219 .217 .214 .212 .210 .208 .205 .203 B
18.4 18.8 19.3 20.0 20.3 20.6 20.9 21.1 21.3 MLT

Plate 5.

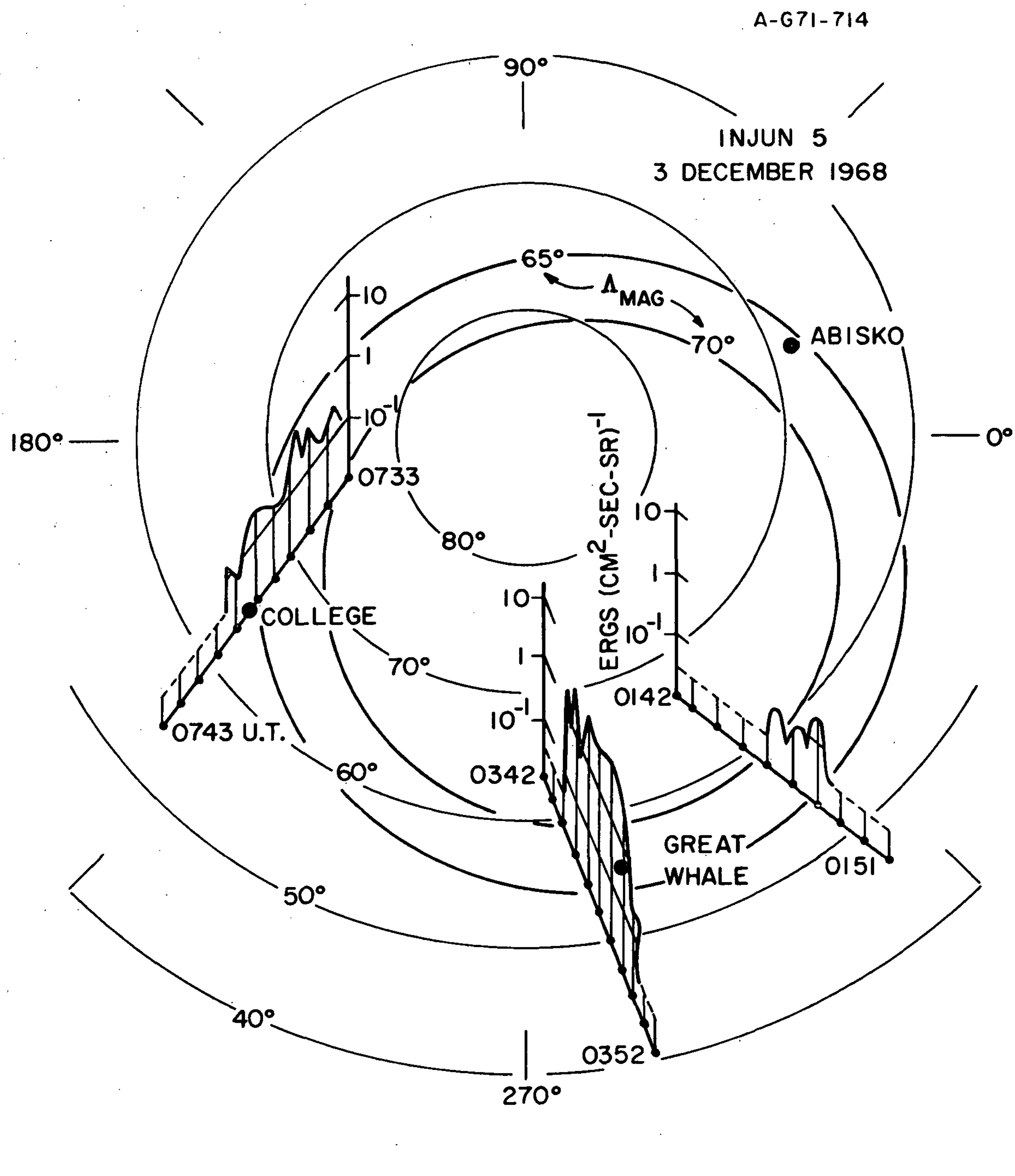

A-G71-714
90°
INJUN 5
3 DECEMBER 1968
65°
Λ_{MAG}
70°
ABISKO
180°
0°
10
1
10^{-1}
0733
80°
$ERGS (CM^2-SEC-SR)^{-1}$
COLLEGE
70°
0142
0743 U.T.
60°
0342
GREAT
WHALE
0151
50°
40°
0352
270°

Figure 1.

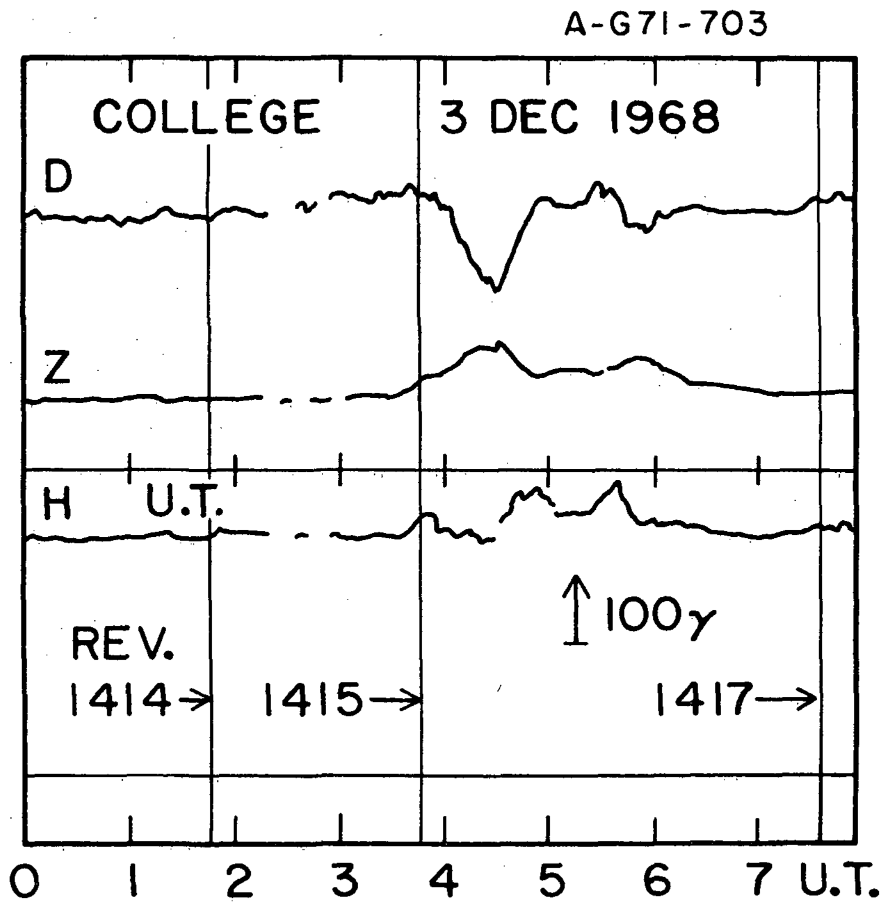
A-G71-703
COLLEGE
3 DEC 1968
D
Z
H
U.T.
100γ
REV.
1414→
1415→
1417→
0
1
2
3
4
5
6
7
U.T.

Figure 2.

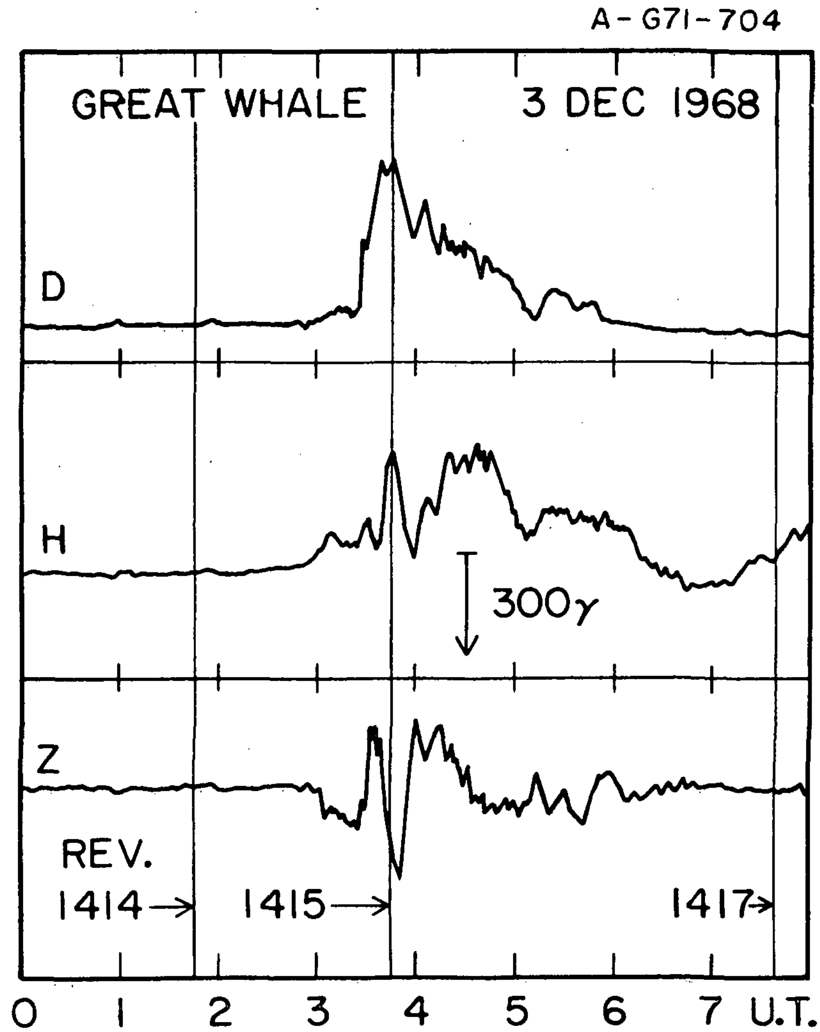
A-G71-704
GREAT WHALE
3 DEC 1968
D
H
300γ
Z
REV.
1414→
1415→
1417→
0
1
2
3
4
5
6
7
U.T.

Figure 3.

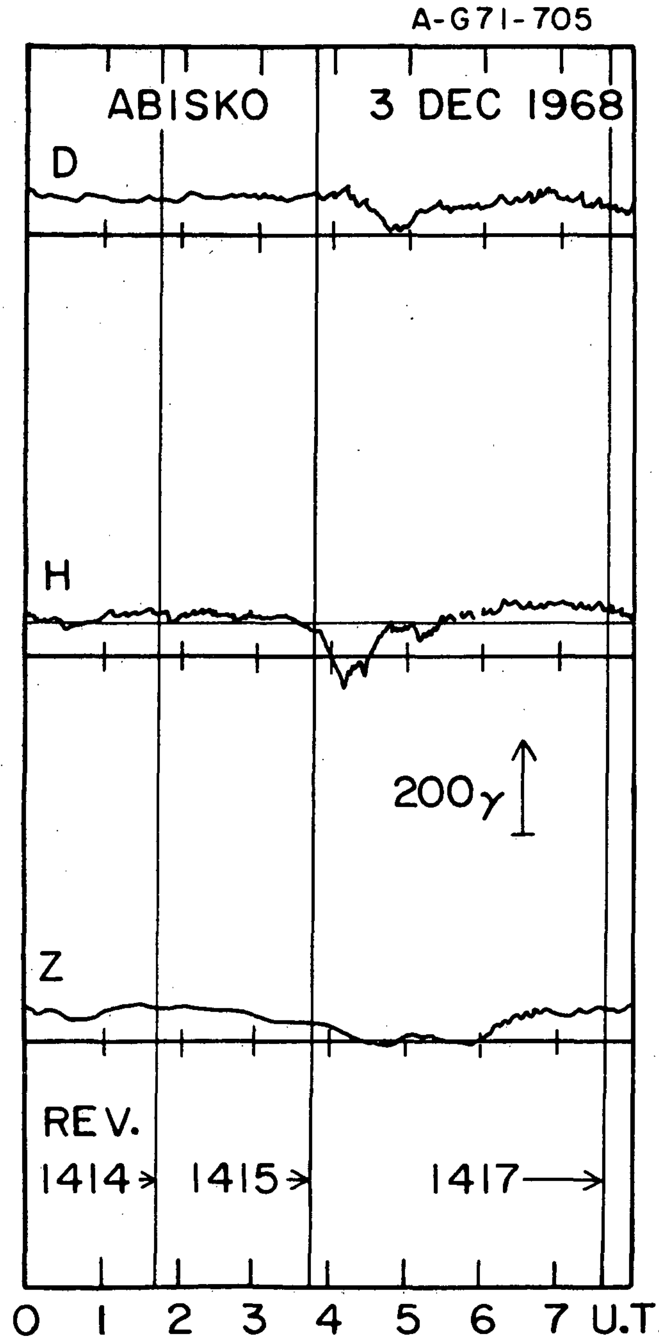
A-G71-705
ABISKO
3 DEC 1968
D
H
200γ
Z
REV.
1414
1415
1417
0
1
2
3
4
5
6
7
U.T.

Figure 4.

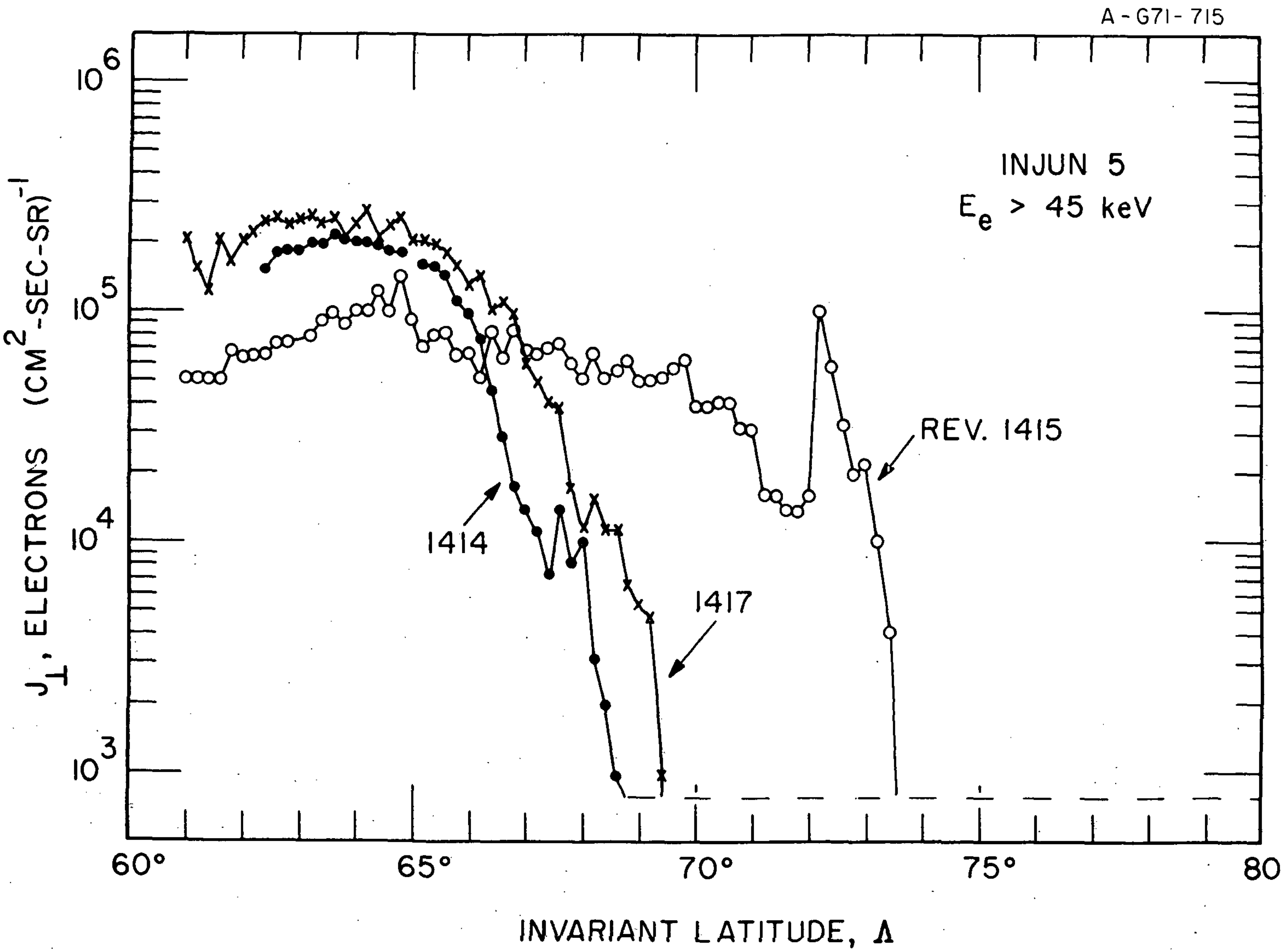
A-G71-715
INJUN 5
E_e > 45 keV
$J_\perp$, ELECTRONS $(CM^2\text{-SEC-SR})^{-1}$
10^6
10^5
10^4
10^3
REV. 1415
1414
1417
60°
65°
70°
75°
80°
INVARIANT LATITUDE, Λ

Figure 5.

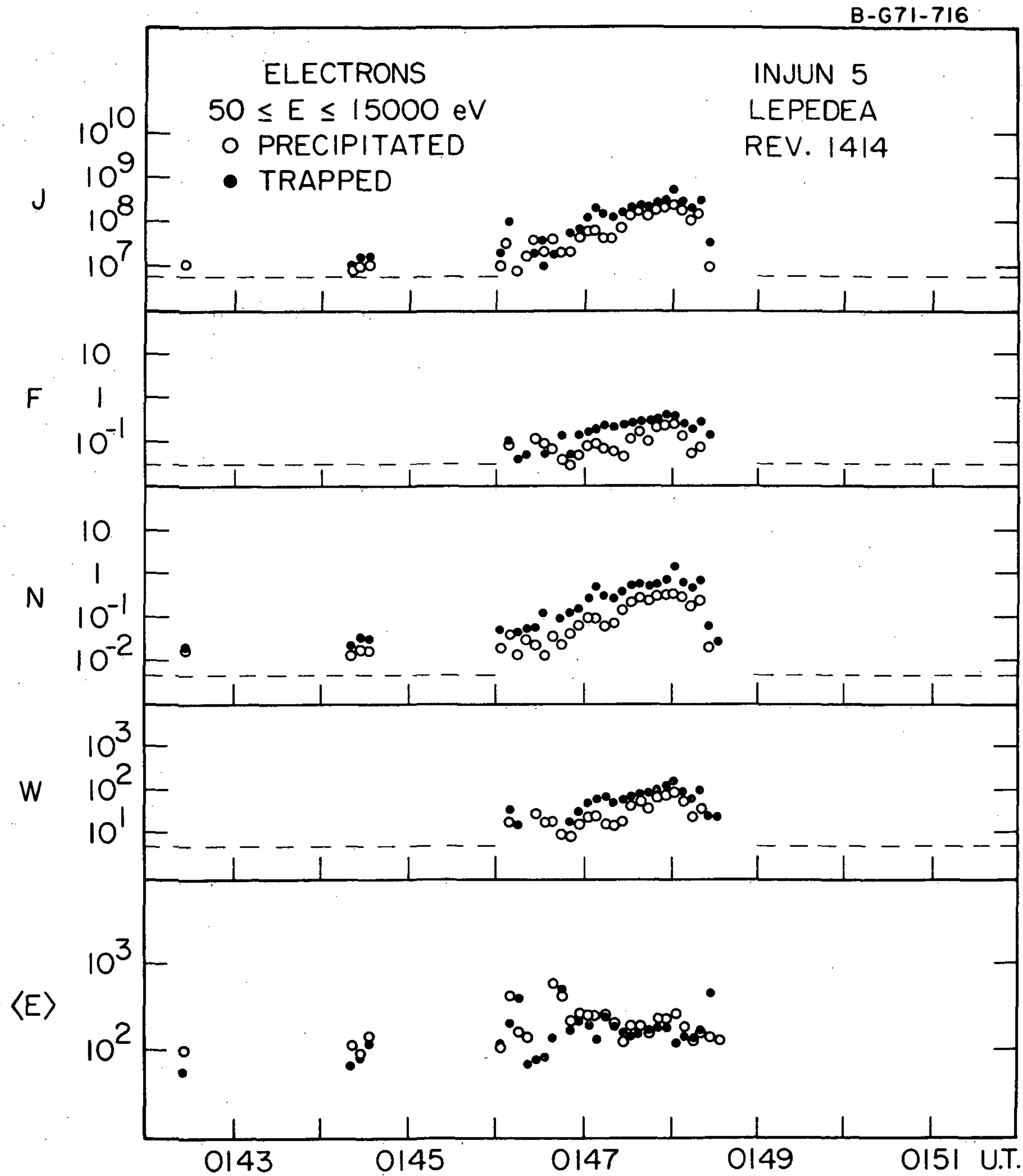
B-G71-716
ELECTRONS
50 ≤ E ≤ 15000 eV
PRECIPITATED
TRAPPED
INJUN 5
LEPEDEA
REV. 1414
J
F
N
W
⟨E⟩
0143
0145
0147
0149
0151 U.T.

Figure 6.

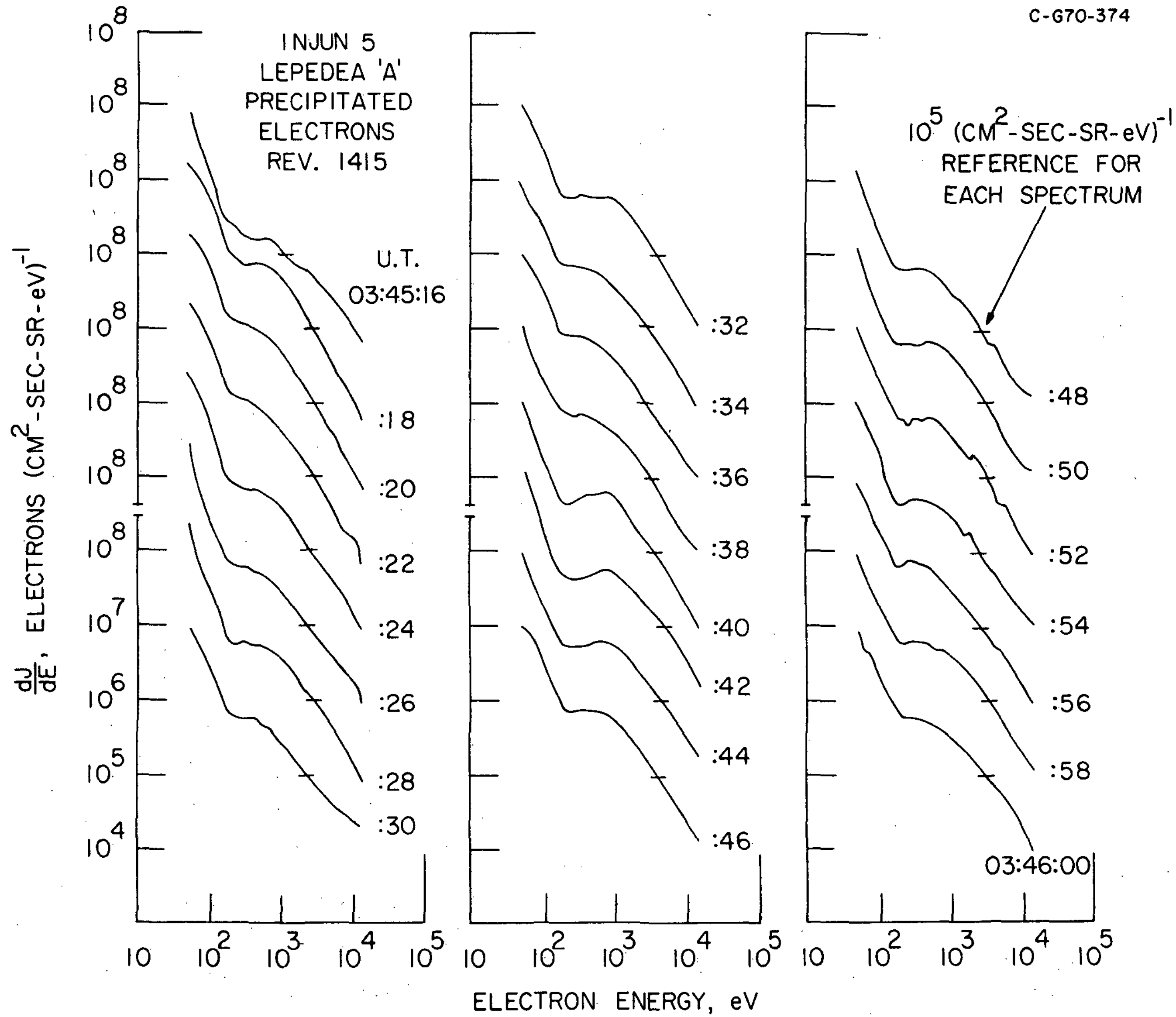
C-G70-374
INJUN 5
LEPEDEA 'A'
PRECIPITATED
ELECTRONS
REV. 1415
U.T.
03:45:16
:18
:20
:22
:24
:26
:28
:30
:32
:34
:36
:38
:40
:42
:44
:46
:48
:50
:52
:54
:56
:58
03:46:00
10^5 (CM^2-SEC-SR-eV)^-1
REFERENCE FOR
EACH SPECTRUM
dJ/dE, ELECTRONS (CM^2-SEC-SR-eV)^-1
ELECTRON ENERGY, eV
10^8
10^7
10^6
10^5
10^4
10
10^2
10^3
10^4
10^5

Figure 7.

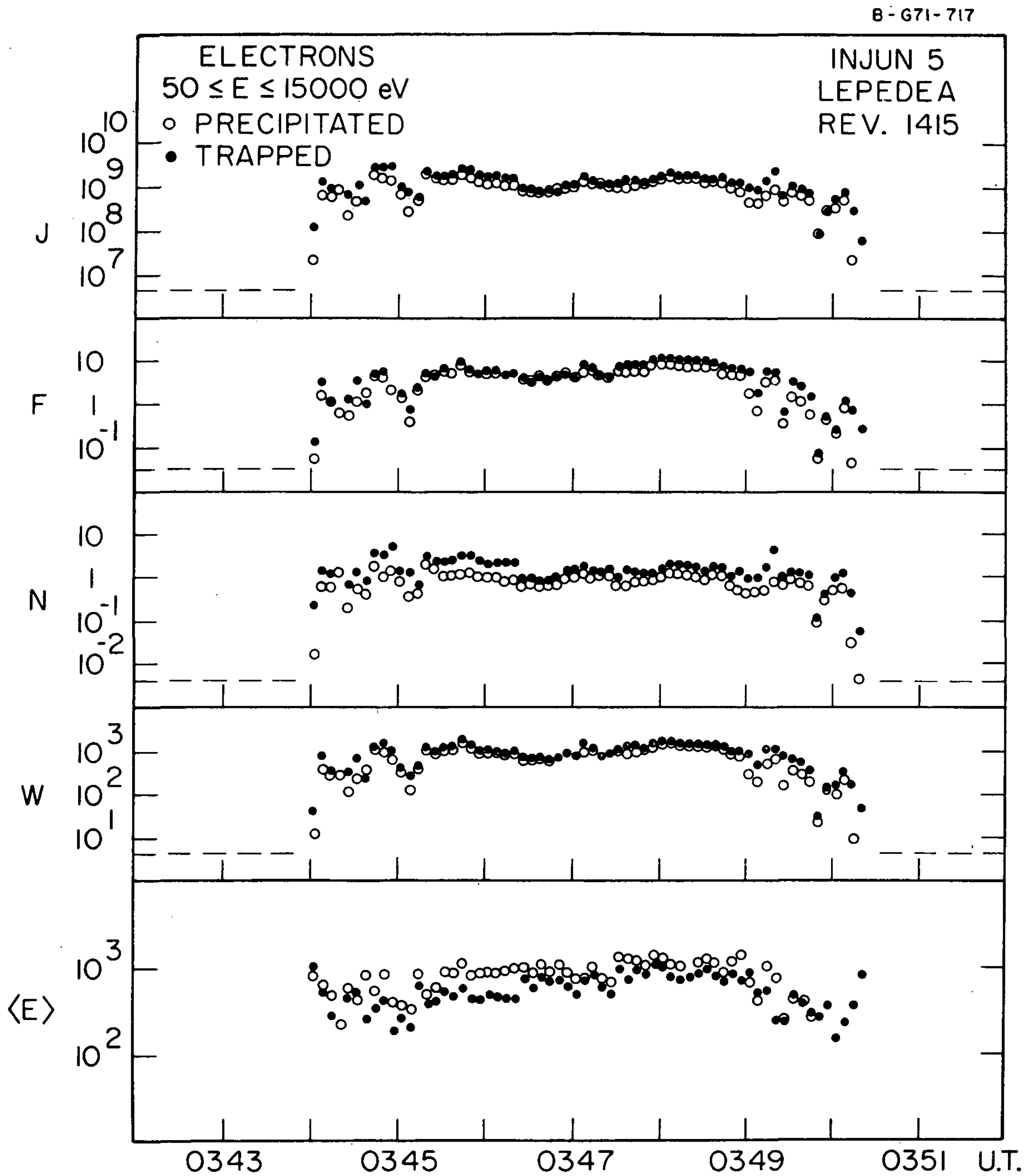
B-G71-717
ELECTRONS
50 ≤ E ≤ 15000 eV
○ PRECIPITATED
● TRAPPED
INJUN 5
LEPEDEA
REV. 1415
J
F
N
W
⟨E⟩
0343
0345
0347
0349
0351
U.T.

Figure 8.

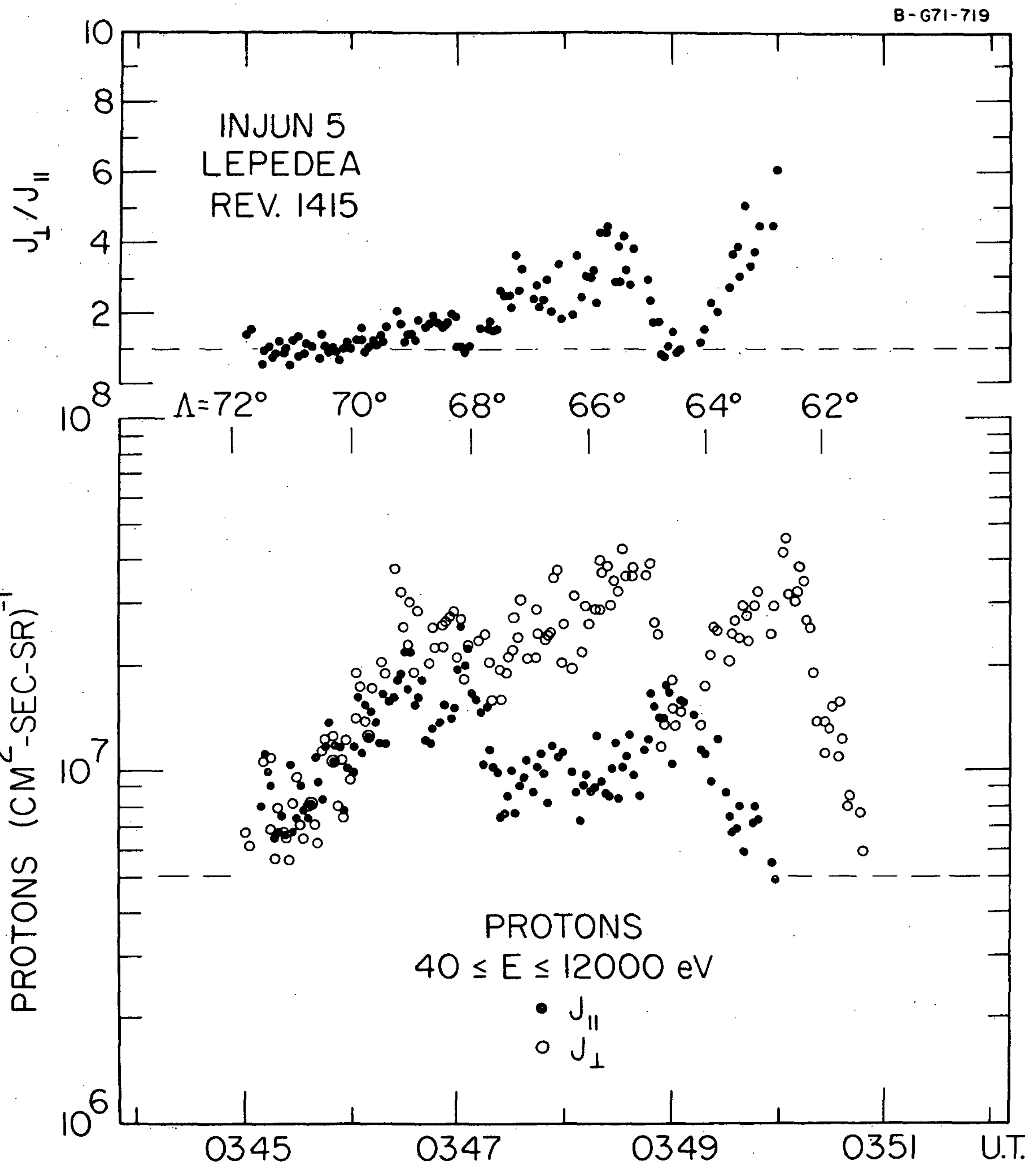
B-G71-719
INJUN 5
LEPEDEA
REV. 1415
$J_\perp/J_\parallel$
Λ=72°
70°
68°
66°
64°
62°
PROTONS (CM^2-SEC-SR)$^{-1}$
PROTONS
40 ≤ E ≤ 12000 eV
$J_\parallel$
$J_\perp$
0345
0347
0349
0351
U.T.

Figure 9.

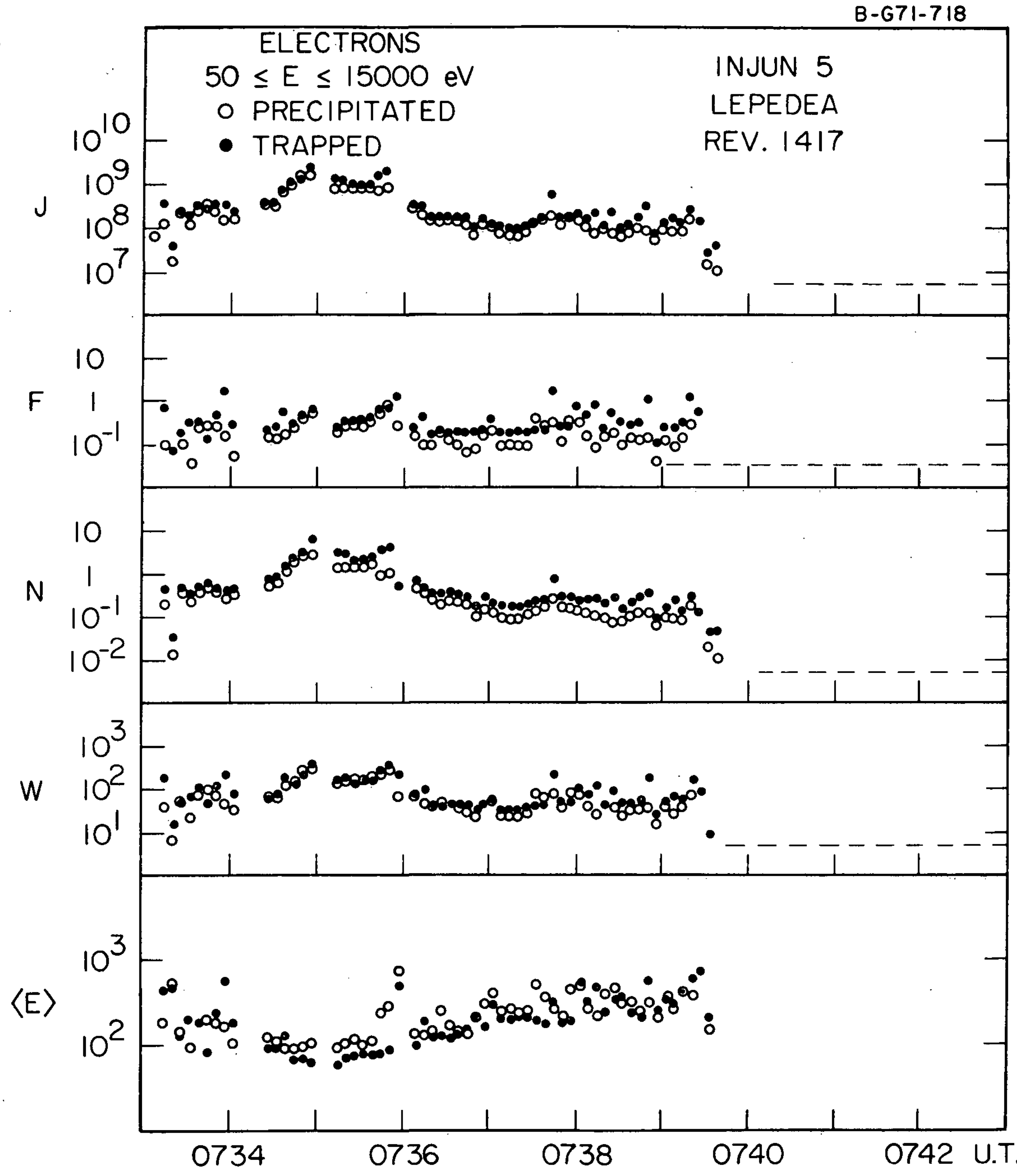
B-G71-718
ELECTRONS
50 ≤ E ≤ 15000 eV
○ PRECIPITATED
● TRAPPED
INJUN 5
LEPEDEA
REV. 1417
J
10^10
10^9
10^8
10^7
F
10
1
10^-1
N
10
1
10^-1
10^-2
W
10^3
10^2
10^1
⟨E⟩
10^3
10^2
0734
0736
0738
0740
0742 U.T.

Figure 10.

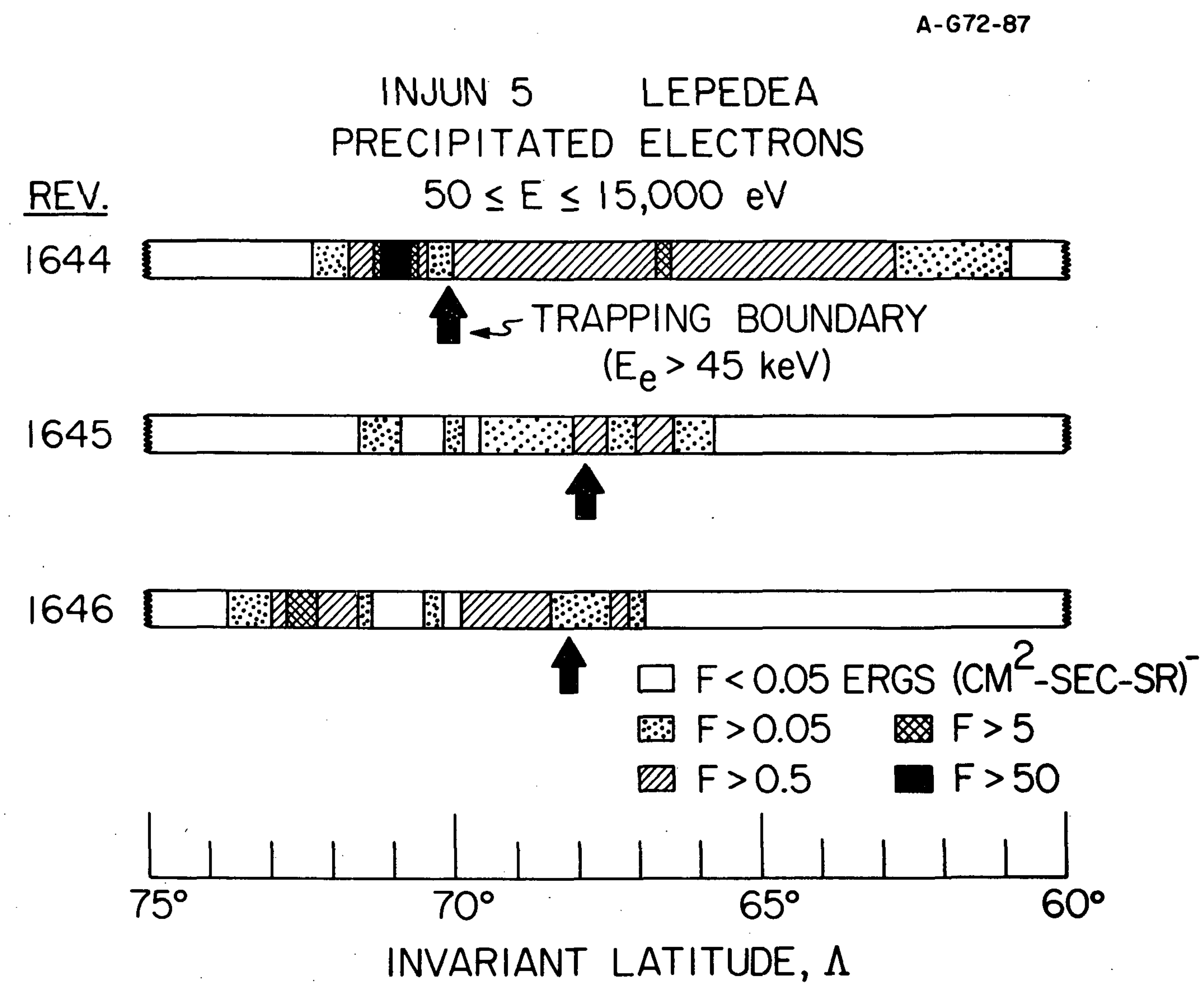
A-G72-87
INJUN 5 LEPEDEA
PRECIPITATED ELECTRONS
50 ≤ E ≤ 15,000 eV
REV.
1644
TRAPPING BOUNDARY
(Ee > 45 keV)
1645
1646
F < 0.05 ERGS (CM2-SEC-SR)-1
F > 0.05
F > 5
F > 0.5
F > 50
75°
70°
65°
60°
INVARIANT LATITUDE, Λ

Figure 11.